ELSEVIER

Cement & Concrete Composites 24 (2002) 281–295

Cement & Concrete Composites

www.elsevier.com/locate/cemconcomp

High-strength concrete and steel interaction in RC members

Maria E. Kaminska

Department of Concrete Structures, Technical University of Lodz, Lodz, Poland

Abstract

A test examining the structural behaviour of beams, slender columns and portal frames subjected to short-term loading is presented. Concrete cube strengths used were 80–100 MPa.

The two reinforcement ratios of beams ($\rho \approx 0.5\%$ and $\rho \approx 1.5\%$), two slenderness ratio of columns ($l/h \approx 12$ and $l/h \approx 22$) and three arrangements of reinforcement of frames (ρ constant) were taken as main parameters of test.

Tests proved that fears of low limit deformability of elements cast of high-strength concrete (HSC) are unfounded.

In elements that failed by crushing of concrete in the compression zone this occurred at much higher strains than those recorded in tests on specimens. In beams strains attained even 6%. Limit curvatures of cross-sections were distinctly greater than in elements cast of normal concrete and full redistribution of internal forces took place in frames. Bond between reinforcement and concrete was retained even at very large strains, exceeding 40‰.

Analytical non-linear model was used to obtain deformation capacity of beams and columns.

Keywords: High-strength concrete; Beam; Column; Frame; Ultimate compressive strain; Curvature; Ductility; Loss off stability; Redistribution of internal forces

1. Introduction

The high-strength concrete (HSC, $f_{ck} > 50$ MPa according to Ref. [1]) is assumed to have low ultimate strain in compression. The collapse of concrete samples is violent, and descending branch of σ–ε diagram is sharper as concrete strength becomes higher. In addition, the procedure of tests (such as strain rate, way of measuring strain, boundary conditions, etc.) is influencing that part of the descending curve.

Strains determined in the tests on specimens are accepted in the codes as mandatory for calculations of elements. Strain ε_{c1} is rising slightly with concrete class, while ε_{cu} diminishes appreciably. For example, according to EC2 [2] for concrete C100/115 both strains become equal, therefore $\varepsilon_{c1} = \varepsilon_{cu} = -0.003$ or $\varepsilon_{c1} = \varepsilon_{cu} = -0.0022$ for parabola–rectangle diagram (ε_{c1} – strain of the peak stress f_c, ε_{cu} – ultimate strain).

Such small ultimate strains of concrete mean appreciable lowering of the design possibilities of cross-section rotation, and that lead to a reduction in the total safety factor. Tests on HSC members do not confirm, however, the limitation on their ductility [3–6].

Investigations presented here are devoted precisely to this problem – deformability of HSC members, subjected to short-term loads. They included eight simply supported beams, 10 slender columns and six portal frames, cast using of concrete of 80–100 MPa cube strength. Present investigations of columns and frames are connected with investigations on ordinary concrete columns and frames carried out earlier in the same laboratory [7,8].

In this paper, a summary of investigation programme is presented, restricted to the results pertaining to problems under consideration. The influence of repeated load, to which all elements were subjected, on strain and load carrying capacity is not discussed. The same applies to the influence of loading history (change of loading planes in columns and reversal of load direction on spandrel beams of frames). All results of tests are presented in [9].

2. Experimental programme and test results

2.1. Simply supported beams

Research included investigation of eight beams - four beams were of rectangular cross-section, and 3000 mm span (defined by support centres) (BP-type). Remaining

0958-9465/02/$ - see front matter
PII: S0958-9465(01)00011-7

beams were of T-shaped cross-section and 5000 mm span (BT-type) (Fig. 1). In both types of beams two ratios of longitudinal tension reinforcement were used (Table 1). Beams marked 'a' were reinforced in the compression zone by 2 bars (∅10 mm, steel class: A-III). Letter 'b' in the symbol stands for the absence of any reinforcement in pure bending compression zone of the beam.

Apart from reinforcement ratios ρ and ρ', Table 1 gives also reinforcement indices (ω, ω_f) which are including the influence of several important variables describing the flexural ductility [10]. The adopted values of ω are distinctly smaller than the maximum allowable in ACI code [11]; this had as the aim creating the possibilities of large strains in concrete and reinforcement in tested elements.

The main measuring process was carried out using linear displacement transducers, which transmitted all the readings, including the pressure in hydraulic system, directly to the computer. During each step of load application, the measuring device recorded 60 readings per second.

Strains on beam faces were measured at two levels: at the top edge, and at 35 mm above the lower edge. Adopted length of measuring bases was 300 mm for BP-beams and 400 mm for BT-beams. The location of measuring bases is shown in Fig. 2.

The beams with higher reinforcement ratio – BP-2 and BT-2 – collapsed as expected, by crushing of the concrete compression zone. In the beams without any reinforcement in the compression zone, the failure was violent, even explosive. The presence of reinforcement in that zone attenuated the whole process.

The views of damaged zones of BP-2a and BP-2b beams are shown in Figs. 3 and 4, respectively. As can be seen, longitudinal reinforcement in the compression zone as well as stirrups restricted the damage zone appreciably, especially with respect to the tension zone.

The destruction of BT-2a and BT-2b beams was of the same character, though not as spectacular.

The development of strain in extreme fibres of the compression zone as a function of load is presented in Fig. 5. It shows the graphs of mean strains from four

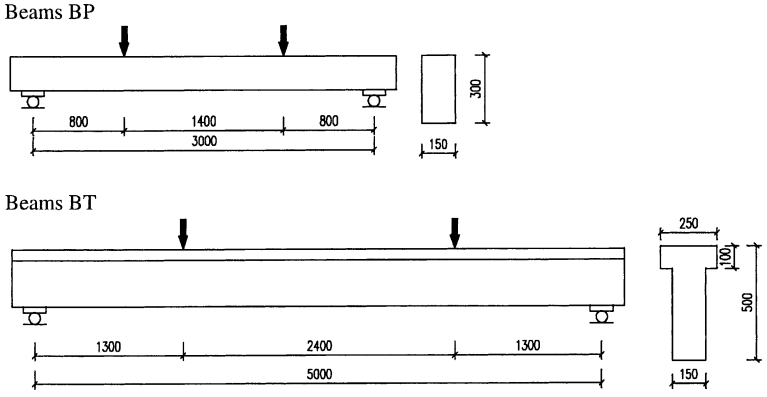

Fig. 1. Cross-sections and dimensions of beams.

Table 1
Characteristics and denotation of the beams[a]

Beam	Longitudinal reinforcement in the zone of pure bending				Reinforcement index $\omega = \frac{A_s f_y - A'_s f_y}{b^* d}$		Stirrup spacing near supports (mm)
	Bottom		Top				
	$\rho = A_s/bd$	Bars	$\rho' = A'_s/bd$	Bars	$\omega(b^* = b)$	$\omega_f(b^* = b_f)$	
BP-1a	0.0038	2∅10	0.0038	2∅10	0		100
BP-1b		2∅10	–	–	0.022		
BP-2a	0.0146	3∅16	0.0039	2∅10	0.060		80
BP-2b		3∅16	–	–	0.086		
BT-1a	0.0048	3∅12	0.0022	2∅10	0.016	0.010	162.5
BT-1b		3∅12	–	–	0.027	0.016	
BT-2a	0.0171	6∅16	0.0023	2∅10	0.090	0.054	75
BP-2b		6∅16	–	–	0.107	0.064	

[a] b: width of web; b_f: width of flange.

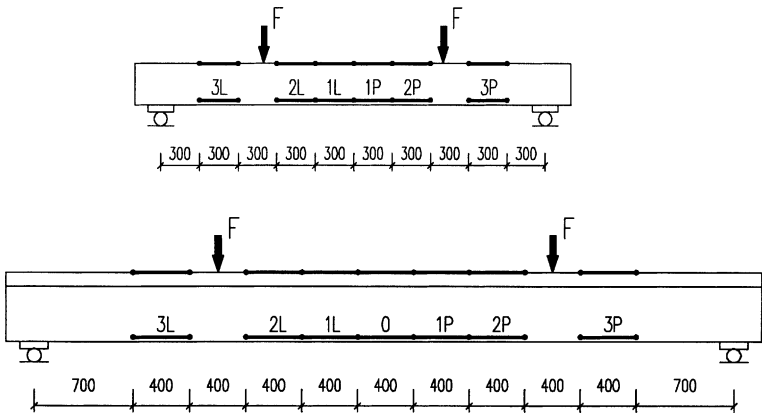

Fig. 2. Location of the bases for measuring the strains in BP and BT beams.

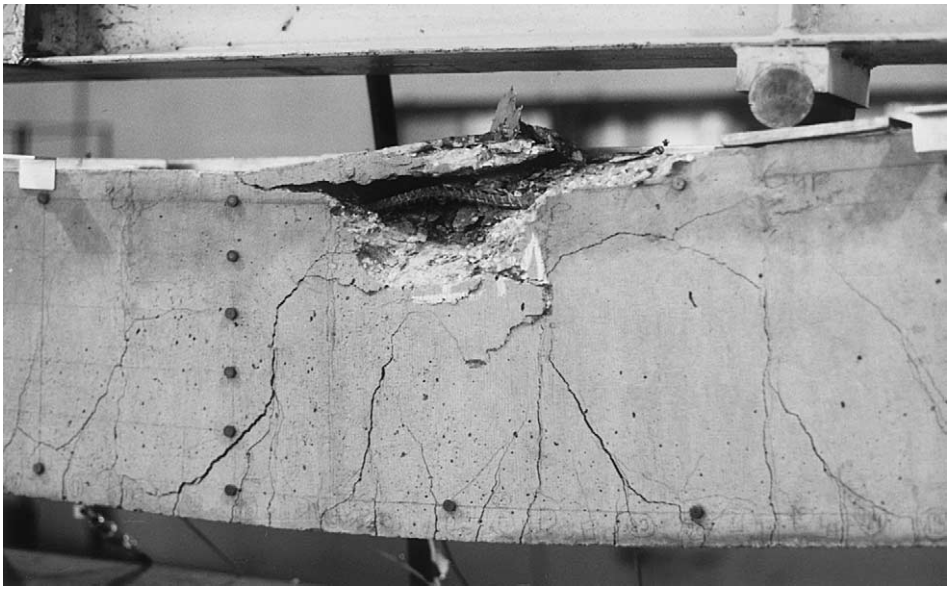

Fig. 3. Beam BP-2a, view of failure zone.

measuring bases on (BP-beams) or five bases on (BT-beams) and maximum strain recorded at a single base.

The destruction (in the sense of material failure) of the beams with low reinforcement percentage (BP-1 and BT-1 beams) has not been reached. Due to the very large deflections, approaching even 200 mm at mid-span, which was beyond the test stand range, further loading of beams was discontinued. Such large displacement was accompanied by large curvatures and very wide cracks. Thus, the beam definitely exceeded the ultimate state of strain.

Graphs showing beam curvatures as functions of load (Fig. 6) indicate large plastic deformation. Graphs show also load increase after yielding of steel, caused by strain hardening effect.

Maximum values of loads and curvatures obtained are presented in Table 2. With respect to highly reinforced beams they refer to the failure load; for beams with low reinforcement ratio they are just the highest obtained in tests. On the ground of strain measurements, load values at which strains in tension reinforcement reached $\varepsilon_s = 10‰$ and $20‰$ were also determined. As can be seen, the limitation of reinforcement strain leads in all cases to lower limit forces than those obtained in investigations.

2.2. Slender columns

Investigation on 10 columns of rectangular cross-section (140×250 mm^2) and 3000 mm length was scheduled (Fig. 7).

Constant longitudinal reinforcement ratio, constant initial eccentricity, two concrete mixes, and two values of column slenderness obtained by applying the load

Fig. 4. Beam BP-2b, view of failure zone.

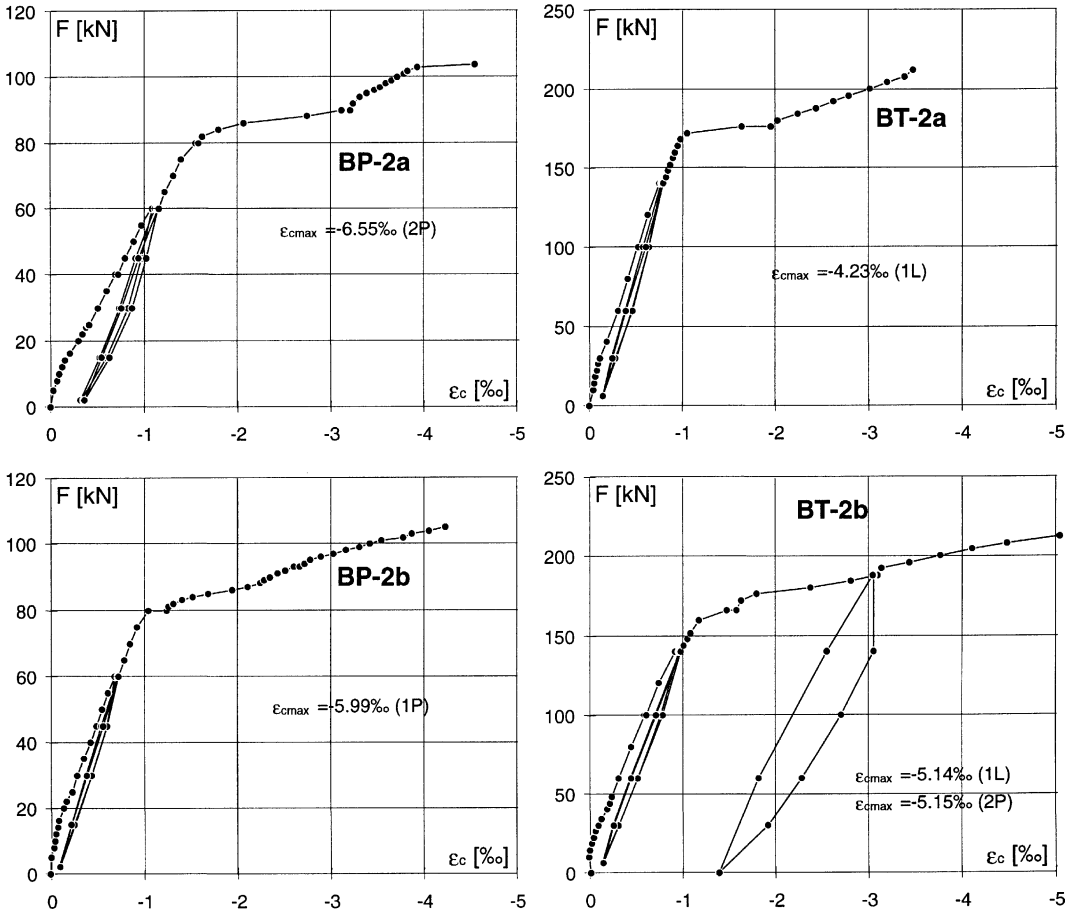

Fig. 5. Development of strain in extreme fibres of the compression zone.

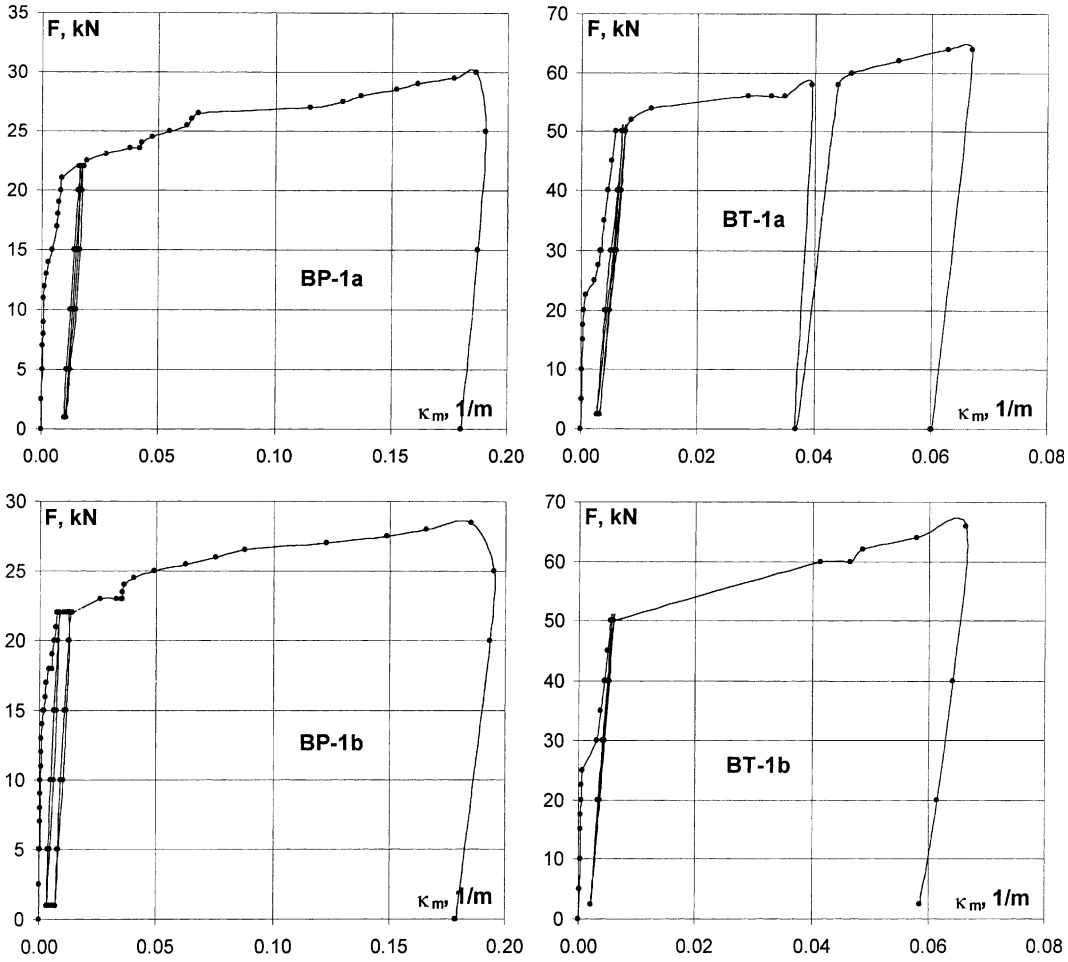

Fig. 6. Curvatures of beams with low reinforcement ratio (the graphs concern pure bending zone).

Table 2
Maximum values of loads and curvature

Beam	$f_{c,cube}$ (MPa)	f_c (MPa)	Load at failure F_u (kN)	Load defined from strain condition F (kN)			Maximum curvature (1/m)
				$\varepsilon_s = 10‰$	$\varepsilon_s = 20‰$	Max.	
BP-1a	93.2	81.2	–	23.5	26.5	30	0.18957
BP-1b	84.6	72.8	–	24.5	26.5	28.5	0.19272
BP-2a	91.6	78.8	104	87.5	100		0.11092
BP-2b	89.5	73.3	105	85.5	98		0.11713
BT-1a	88.6	72.5	–	55.2	60	64	0.06702
BT-1b	87.6	78.0	–	56	60	66	0.06677
BT-2a	87.9	73.3	212	176	200		0.06434
BT-2b	78.6	70.3	212	183	205		0.06073

alternatively in two planes of symmetry were assumed. All symbols and element characteristics are shown in Table 3.

'Sw' and 'Sk' symbols inform in which plane column is destroyed. Columns marked Sw were loaded in the plane of lesser stiffness, and these marked Sk – in plane of greater stiffness.

'A' in column symbol stands for load applied in a single stiffness plane until the collapse of the column. 'B' denotes that the load was applied in first stiffness plane up to a certain level. Then the load was relieved and applied in the second plane until the column collapse.

Fig. 8 explains the way of applying the loads. Initial load eccentricity was always equal to 50 mm.

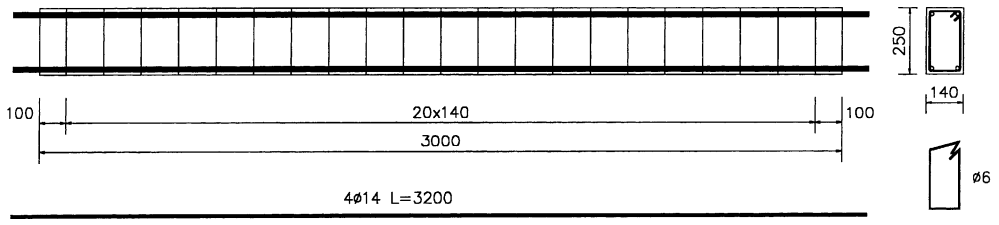

Fig. 7. Column reinforcement.

Table 3
Symbols and properties of specimens

Column	Cross-section $b \times h$ (mm)	Column slenderness (l/h)	Relative eccentricity (e/h)	Concrete $f_{c,cube}$ (MPa)	Stirrups spacing (mm)
Sw-1A				90	
Sw-1B	250 × 140	21.4	0.36		
Sw-2A				100	
Sw-2B					140
Sk-1A				90	
Sk-1B	140 × 250	12.0	0.20		
Sk-2A				100	
Sk-2B					
Sw-2Ac	250 × 140	21.4	0.36	90	70
Sk-2Ac	140 × 250	12.0	0.20	90	

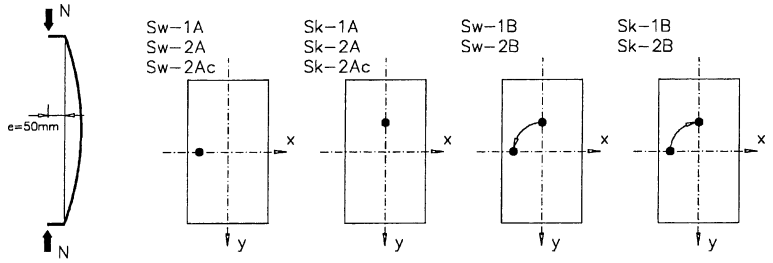

Fig. 8. Rules of applying the loads to the columns.

Numbers 1 and 2 are referring to concrete strength ($f_{c,cube} = 90$ and 100 MPa, respectively); 'c' in the symbol of the last two columns indicates the application of stirrups with welded ends at half the spacing used in the remaining columns.

All columns were loaded in vertical position in a Class 1.0 hydraulic press of 6000 kN capacity. Two of its ranges were used: up to 600 kN and up to 2000 kN.

Overall view of the test stand is shown in Fig. 9.

During the test the displacements of column axis and strains on column surfaces were taken.

Special measuring system, used in previous tests was applied to measure displacements. In all columns displacements were recorded at three cross-sections along column height (Fig. 10) by means of linear displacement transducers. Strains on the surface of concrete were determined too by means linear transducers at five measurement bases over the height of the column (Fig. 10).

The situation of neutral axis of strain in the cross-sections of two columns is shown in Fig. 11 for selected longitudinal forces. The values of these forces, as well as the values of corresponding strains are given in the drawings. It can be noticed that neutral axes of strain are not perpendicular to straight lines determining the theoretical axis of load, i.e., the neutral axis. This can be assigned to incidental, unintentional eccentricities occurring during investigations.

Two models of column failure occurred in tests. They were connected with the direction of ultimate load plane.

Sw-type columns in which the failure occurred in the plane of lesser stiffness, failed because of the loss of stability. The growth of column deflections made their

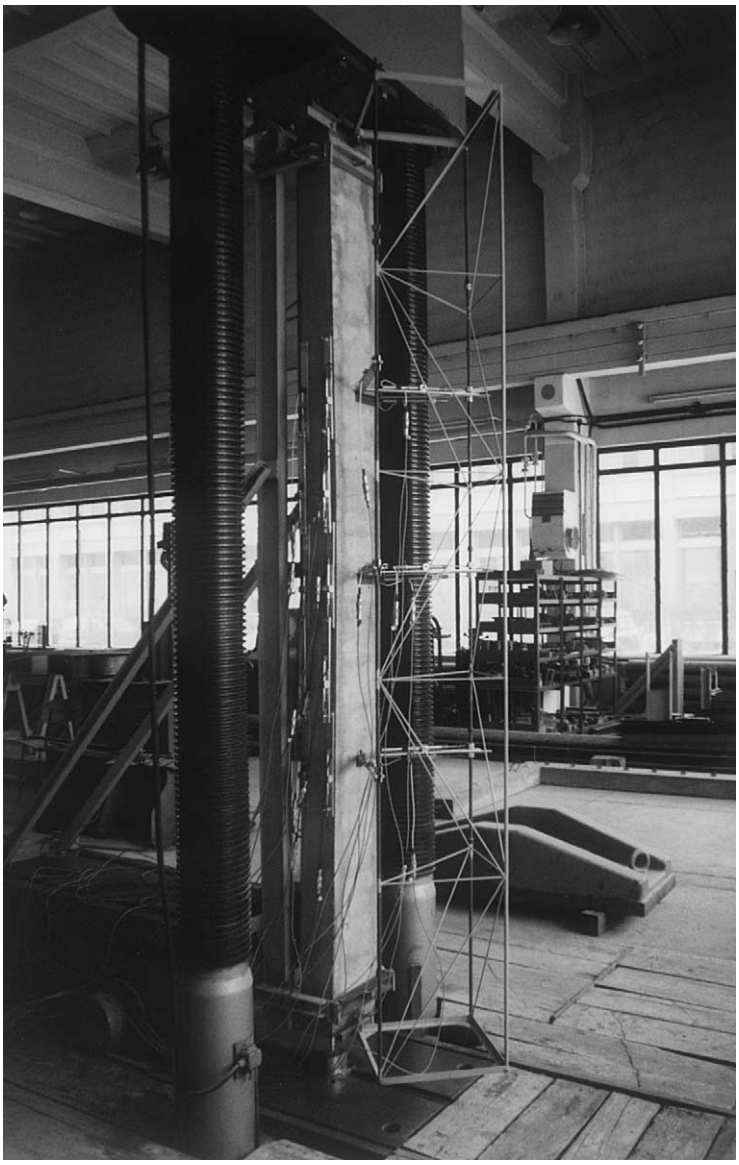

Fig. 9. Overall view of test stand. Truss construction for measuring displacements is visible.

further loading impossible. The development of deflections in these columns as functions of load is shown in Fig. 12 on the example of columns Sw – 1A and Sw – 2Ac.

Sk-type columns loaded in the plane of greater stiffness failed by crushing of concrete in compression zone. The failure had a very violent character, concrete burst and reinforcing bars buckled.

The cause of failure in individual columns, magnitude of forces at failure and strains in the extreme fibre of the compression zone at the maximum force attained in test is presented in Table 4.

It is worth noticing that buckling of the columns occurred at similar strains of the extreme fibre of the compression zone, independent of class of concrete (1 or 2) or stirrup spacing.

In columns types Sk-2A and Sk-2B, in which concrete was crushed at column mid-height, strain in the extreme fibre of the compression zone exceeded 4‰. The influence of stirrup spacing proved here advantageous: strain at failure in column Sk-2Ac was $\varepsilon_c = -5.78‰$.

2.3. Portal frames

Dimensions, static diagram and loading procedure of frames were adopted as in Fig. 13.

Constant system of reinforcement over the length of beam and columns was assumed. Total reinforcement ratio was about 0.018. Reinforcement was, however, assigned in a different way to inner and outer sides of the frame so, as to force distinct redistribution of internal forces.

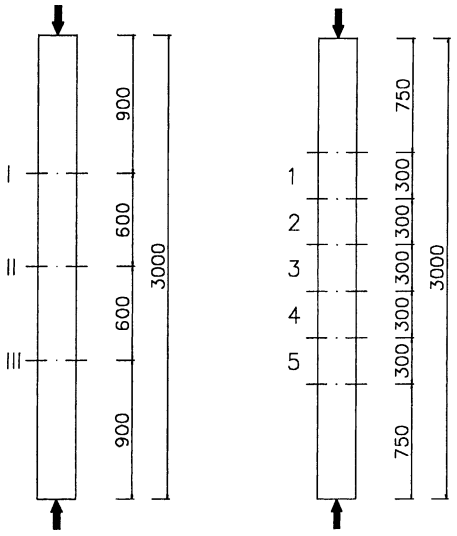

Fig. 10. Situation of cross-sections at which column axis displacements were determined and layout of strain measurement bases on concrete surface.

Symbols of frames and distribution of reinforcement is explained in Table 5. Symbol RPW-a/b denotes frames having reinforcement at the inner side stronger than at the outer edges; symbol RPW-b/a refers to reinforcement arranged in opposite way.

For RPW-c/c frames, symmetrical reinforcement was assumed, corresponding to moment diagrams defined for materials of linear-elastic characteristics.

As follows from Fig. 13, loading of frames was provided for two stages, with change of load direction. In the first stage, two loading levels were assumed (numbers 1 and 2 in frame symbols refer to this). In stage II of loading, loading up to failure (destruction of material or state of excessive displacement) was assumed.

Reinforcement layouts in one of frame types adopted are shown in Fig. 14. At frame corners the reinforcement was so arranged, as to allow for moment sign reversal.

Frames were tested in horizontal position on a specially prepared test stand (Fig. 15).

Displacements of axes of frame members, changes in length of distances connecting frame nodes and reactions at supports were measured during investigations. Observations of crack maps and their development were also carried out.

In four unsymmetrical reinforced frames, the failure was by crushing of concrete in compression zones, al-

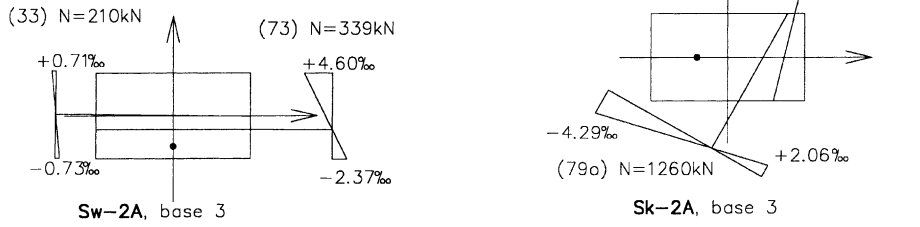

Fig. 11. Change in the position of the neutral axis and strains in extreme fibres of the cross-section.

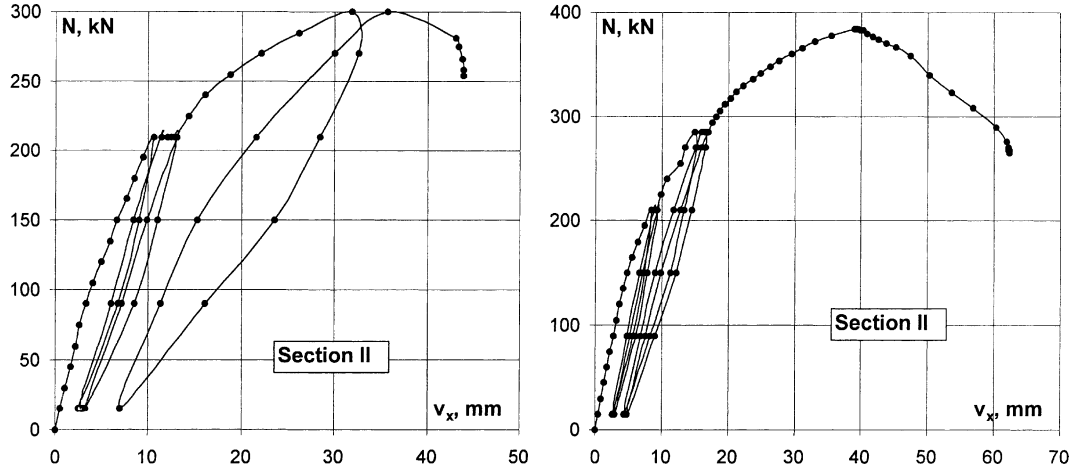

Fig. 12. Deflections of Sw-1A and Sw-2Ac columns as functions of load.

Table 4
Mode of failure and experimental values of $N_{u,test}$ and ε_c

Column	$f_{c,cube}$ (MPa)	f_c (MPa)	$N_{u,test}$ (kN)	Strain ε_c ‰	Base	Mode of failure
Sw-1A	98	66[a]	300	−2.46	3	Loss of stability
Sw-1B	95	81	330	−2.56	3	
Sw-2A	100	88	339	−2.37	3	
Sw-2B	100	76	384	−2.15	3	
Sk-1A	96	84	1300	−3.61/−3.95	2/4	Crushing of concrete
Sk-1B	91	65[a]	1180	−3.15/−3.45	2/4	close to column cap
Sk-2A	99	83	1270	−4.28	3	Crushing of concrete at
Sk-2B	102	81	1300	−4.17/−4.31	3/4	column mid-height
Sw-2Ac	107	80	384	−2.48	3	Loss of stability
Sk-2Ac	110	99	1300	−5.78	3	Crushing of concrete

[a] Specimen bases were smoothed using gypsum; in the remaining cases specimens were capped.

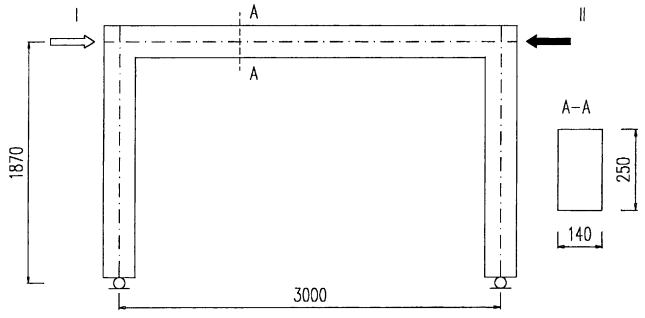

Fig. 13. Dimensions, static diagram and loading procedure.

ways at two cross-sections: in column under tension and at the corner under tension on the outer side. In two remaining frames with symmetric reinforcement, load increase was stopped in view of very large displacements and – in the first place – because rotations at supports, which risked that the element would lean on buffer stops.

Values of maximum forces attained in tests together with values of repeatable loading in first and second loading stages are presented in Table 6.

When analysing the values of the maximum load on frames, it can be noticed, that highest loads were carried by RPW-c/c frames, despite somewhat lower total reinforcement ratio than in the remaining frames; this load did not yet cause the exhaustion of carrying capacity of cross-sections.

The horizontal reaction values showed very distinct redistribution of internal forces in frames with unsymmetrical reinforcement. Final degree of redistribution, at simultaneous failure of two sections, was about $\delta = 0.48$ in frames RPW-a/b-1 and RPW-a/b-2 and $\delta = 0.90$ in frame RPW-b/a-2. No reliable result was obtained in case of frame RPW-b/a-1.

In frames with symmetrical reinforcement (RPW-c/c), redistribution of internal forces took place only at loads over $F = 35$ kN. Maximum degree of internal force redistribution amounted to about $\delta = 0.84$ in frame RPW-c/c-1 and $\delta = 0.87$ in frame RPW-c/c-2. In both cases the reason for breaking off load increase were very large displacements and not the state of material destruction.

Displacements in frames were the reflection of internal force configuration, changing with the increasing load. This is particularly visible in diagrams of displacements of RPW-a/b frames (Fig. 16). The graphs have been prepared for maximum forces in the first stage of loading (dotted line), for corresponding forces in second stage, as well as for the maximum load.

From displacement graphs of column axes it can also be observed which column cross-sections failed by crushing of concrete. Destruction zone is visible as a loss of smoothness in displacement graph.

Table 5
Specimens reinforcement data

Specimen	Longitudinal reinforcement		Reinforcement ratio		
	Inner	Outer	Inner	Outer	Total
RPW-a/b-1	2∅14	2∅10	0.013	0.005	0.018
RPW-a/b-2	+1∅12				
RPW-b/a-1	2∅10	2∅14	0.005	0.013	0.018
RPW-b/a-2		+1∅12			
RPW-c/c-1	2∅12	2∅12	0.0085	0.0085	0.017
RPW-c/c-2	+1∅8	1 + ∅8			

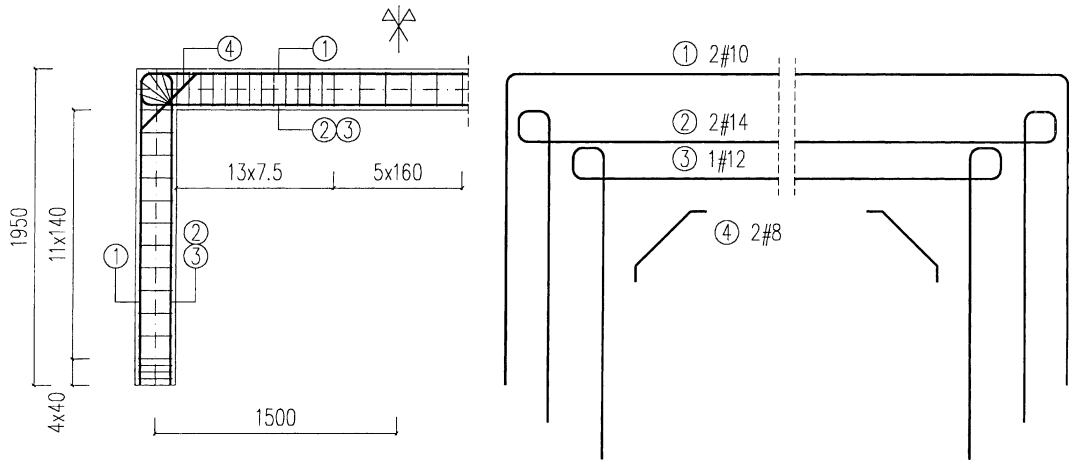

Fig. 14. Reinforcement of the RPW-a/b frames.

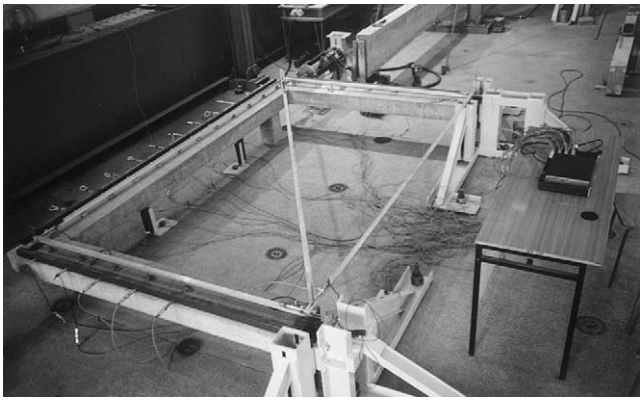

Fig. 15. Overall view of the test stand.

Crack maps after ending the test are shown in Fig. 17. Cracks formed in the first stage of loading, which closed after the change of load direction, are drawn using thin line in developments of frame side elevations.

The picture of cracks after the end of loading, confirms earlier observations on full redistribution of internal forces in frames RPW-a/b and RPW-b/a, manifested by simultaneous reaching of the limit of capacity at two cross-sections.

3. Discussion of the results

The test proved that there exists a difference in behaviour of HSC in structural elements and in specimens, favourable from the point of view the structural safety. This remark applies to all types of investigated elements: beams, columns and frames.

Limit strains of the compression zone at crushing of concrete amounted to 4.2‰ and 6.5‰ – twice as much as in specimen cube tests. In columns, the analogous strains were of the order of 4.5‰ and – with closer spacing of stirrups – even 5‰. These strains do not therefore differ from strains obtained in ordinary concrete elements.

For the purposes of analytic calculations the model of concrete, analogous to that of ordinary concrete (Fig. 18) was used. It is described using relations (1)–(6) in function of $f_{c,cube}$ [12]:

$$f_c = [0.83 - 0.01\ \ln(t_m)]f_{c,cube} \quad (\text{MPa}), \tag{1}$$

$$\varepsilon_{c1} = [0.0075 f_{c,cube} + 0.125\ \ln(t_m) + 1.655]10^{-3}, \tag{2}$$

$$\sigma_c = f_c \frac{\beta(\varepsilon_c/\varepsilon_{c1})}{\beta - 1 + [\varepsilon_c/\varepsilon_{c1}]^{\beta}}, \tag{3}$$

Table 6
Repeatable and maximum loads on frames

Frame	$f_{c,cube}$ (MPa)	f_c (MPa)	Repeatable loading (kN)	Maximum loading (kN)	Cause of ending the test
RPW-a/b-1	107	93	20	42	Crushing of concrete at two cross-sections
RPW-a/b-2	110	88	26	44	
RPW-b/a-1	97	85	20	42	
RPW-b/a-2	119	85	26	43	
RPW-c/c-1	102	88	20	44	Excessive displacements and rotations
RPW-c/c-2	106	87	30	45	

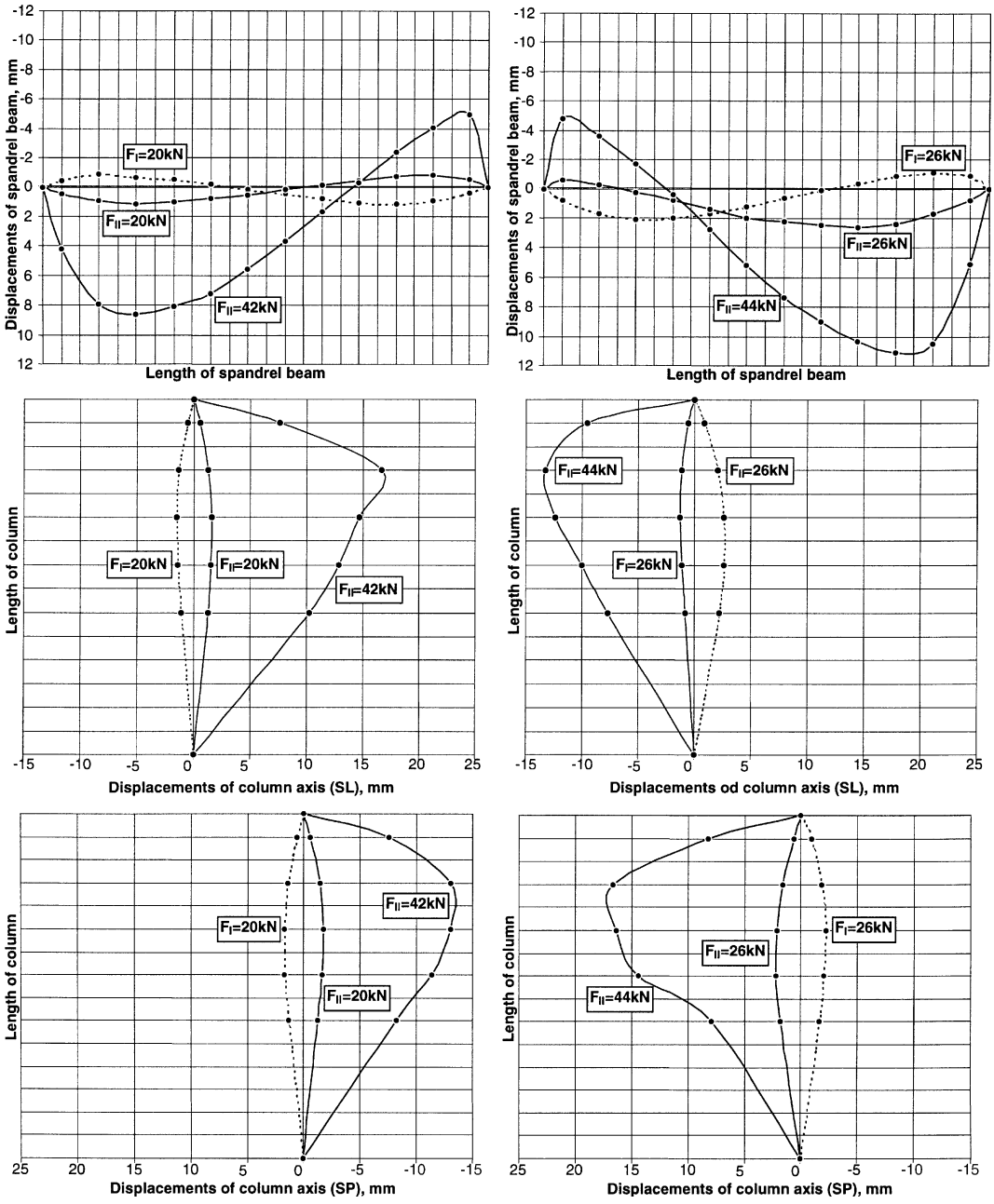

Fig. 16. Displacement diagrams for beam and both column axes in RPW-a/b-1 and RPW-a/b-2 frames (SL – left column; SP – right column).

$$\beta = \frac{1}{1 - (f_c/(\varepsilon_{c1}E_c))}, \tag{4}$$

$$E_c = E_{c0}[0.99 - 0.0158\ \ln(t_m) - 0.0013 f_{c,cube}] \quad (\text{MPa}), \tag{5}$$

$$E_{c0} = 4.03(2300 + 3.17 f_{c,cube})(f_{c,cube})^{1/3} \quad (\text{MPa}), \tag{6}$$

where t_m: time (minutes) when the strain increases of 1‰.

Principles of tension stiffening and smeared cracking were applied with relation to reinforced concrete tension zones.

The cross-section is considered first in calculations, adopting the principle of plane sections remaining plane and determining the relationship moment–curvature. Subsequently, a member is considered, integrating the curvature along its length, taking account of boundary conditions and second-order effects.

Applying this method of analysis to investigated elements, a very good agreement was obtained of

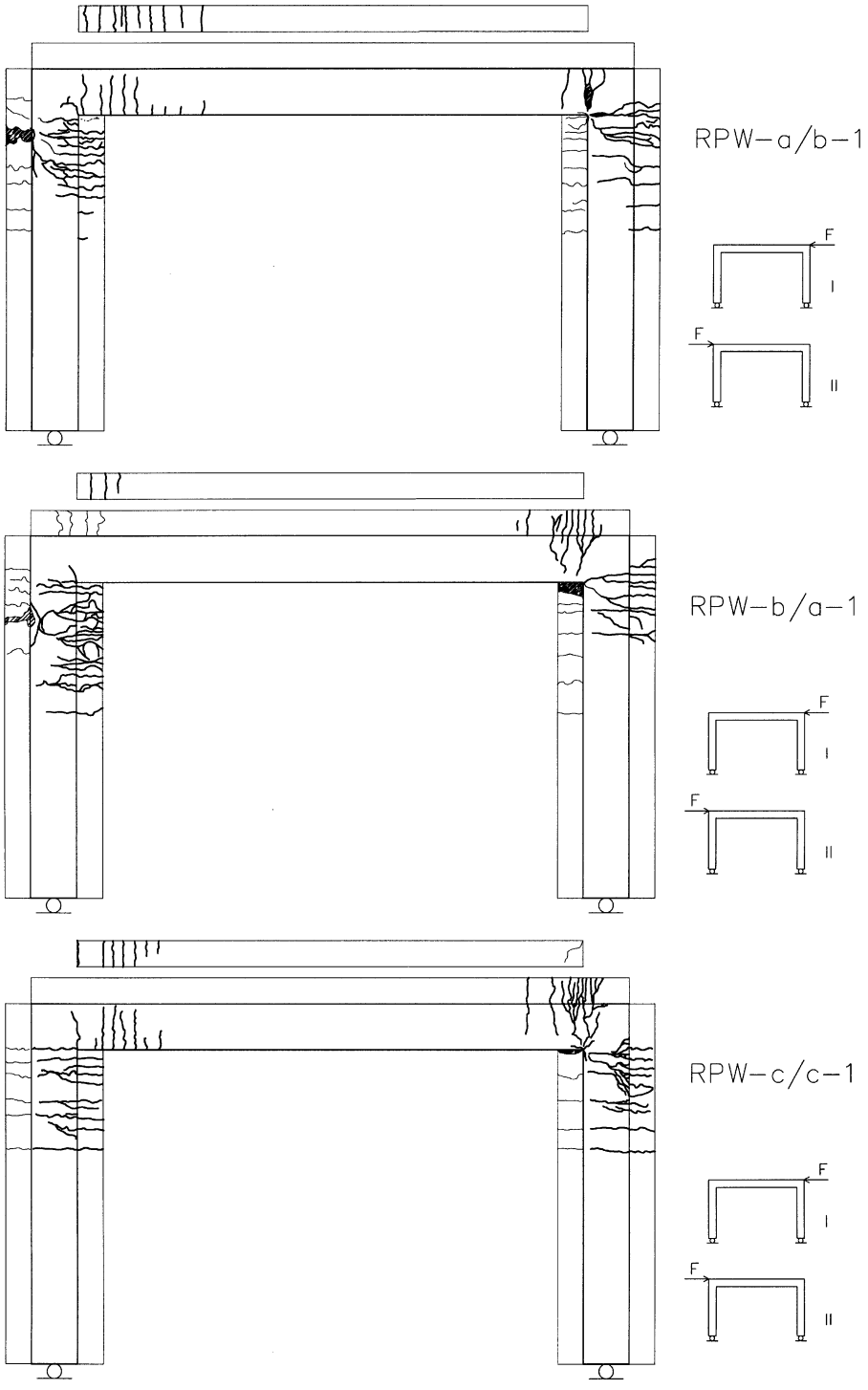

Fig. 17. Crack map of frames loaded up to the lower load level during the first stage of tests.

theoretical and empirical values – e.g., with relation to columns – $N_{u,cal}/N_{u,test} = 1.01$, at standard deviation $\delta = 0.014$.

This justifies making some numerical simulations. Influence of the reinforcement ratio on flexural ductility was analysed with reference to cross-section of beam. Rectangular cross-section was considered, reinforced in the tension zone only, at $d = 0.9h$. Two values of concrete strength were adopted: $f_{c,cube} = 30$ and 100 MPa, $t_m = 60$ min, and reinforcing steel of elastic–plastic characteristic ($f_{yk} = 410$ MPa, $E_s = 200$ GPa). Computations results are presented in the

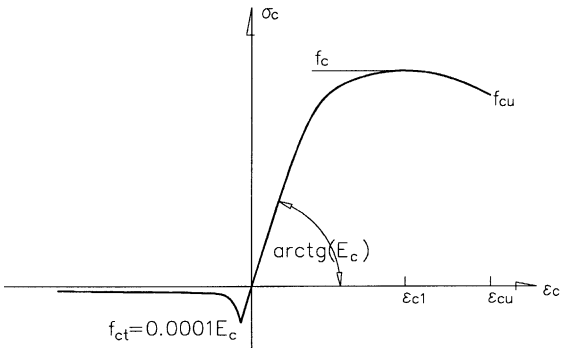

Fig. 18. Concrete constitutive laws after Czkwianianc and Kaminska [10].

form of moment–curvature relationship, in reduced form (moment $m = M/bh^2$, curvature κh, Fig. 19). Values of the reduced curvature of strain limitation of the tensile reinforcement to $\varepsilon_s = 10‰$ or the extreme fibre of the compression zone to $\varepsilon_{cu} = -3.5‰$. If the reinforcement ratio amounts to $\rho = 0.0015$, then at $f_{c,cube} = 100$ MPa the cracking moment is slightly less than the yield moment of steel and, after cracking, the tangent stiffness diminishes rapidly. In case of ordinary concrete the cracking moment amounts to about 80% of the yield moment of steel and tangent stiffness diminishes more slowly. At the reinforcement ratio $\rho = 0.004$, the relations between the cracking moment and yielding moment are similar for both types of concrete. The loss of stiffness after cracking is also similar. At high reinforcement ratio, advantageous influence of concrete strength on stiffness and bending capacity of members becomes noticeable.

With reference to columns, the calculations confirmed observations concerning the destruction due to loss of stability. Computations were made for rectangular section with reinforcement ratio $\rho = \rho' = 0.01$, assuming $a/d = 0.1$ and $f_{c,cube} = 100$ MPa. Three slenderness ratios were examined: $l/h = 10$, 20, 30, as well as three relative initial eccentricities: $e = 0.1h$, $0.3h$, $0.5h$, constant over the entire column length (Fig. 20).

As can be noticed, in two cases the graphs of N–M relationship, describing the behaviour of a slender column under load, attain the maximum before the cross-section point with the curve determining the load carrying capacity of cross-section. This refers to the initial eccentricity $e = 0.5h$ at slenderness ratios $l/h = 10$ and 20. The graphs prove, however, that the loss of carrying capacity of column due to loss of stability is insignificant. Situation is similar by the increase of initial eccentricity, as shown in Fig. 21.

For comparison, an analogous computation was carried out assuming $f_{c,cube} = 30$ MPa at initial force eccentricity $e = 0.75h$. In this case the computations also indicate the possibility of columns failure due to loss of stability.

4. Conclusions

The experimental results and the calculations discussed in the present paper obtained ascertain the following remarks:

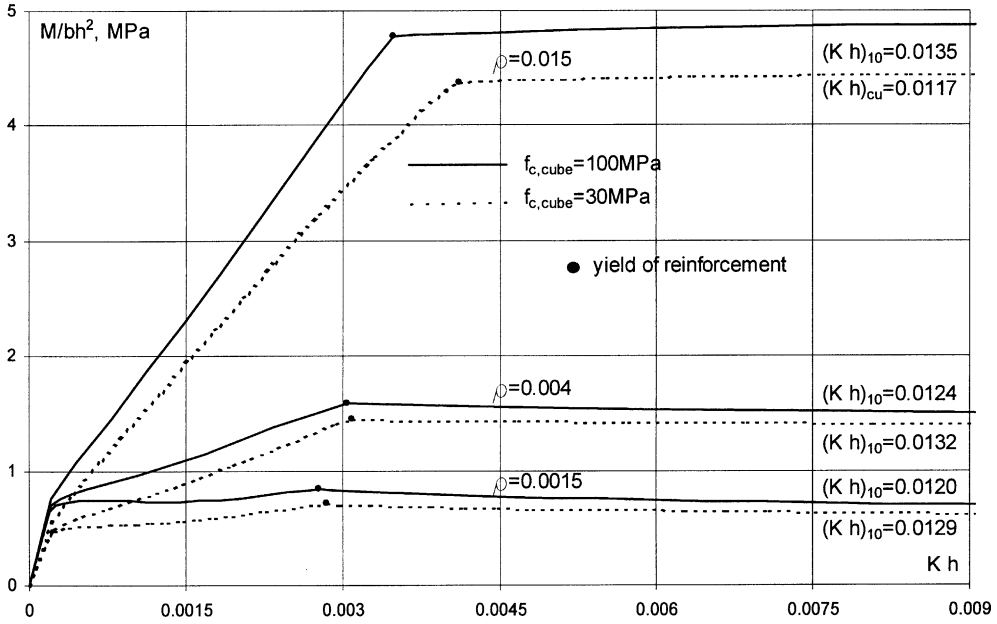

Fig. 19. Calculation moment–curvature relationships as function of reinforcement ratio.

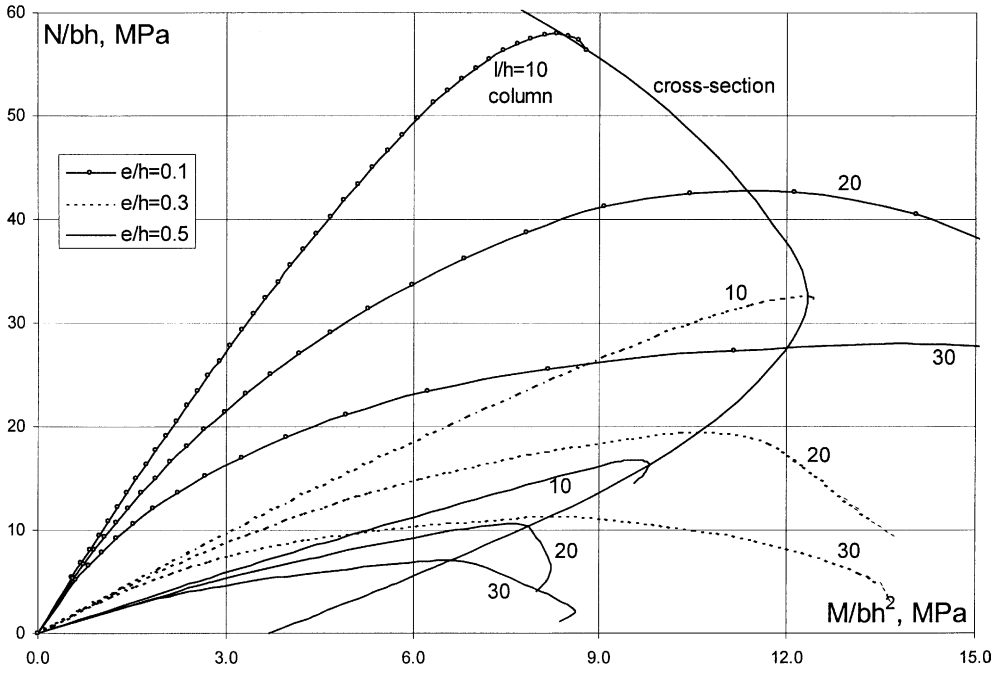

Fig. 20. Calculation analysis of load-bearing capacity of columns, $e = 0.1h$, $0.3h$, $0.5h$.

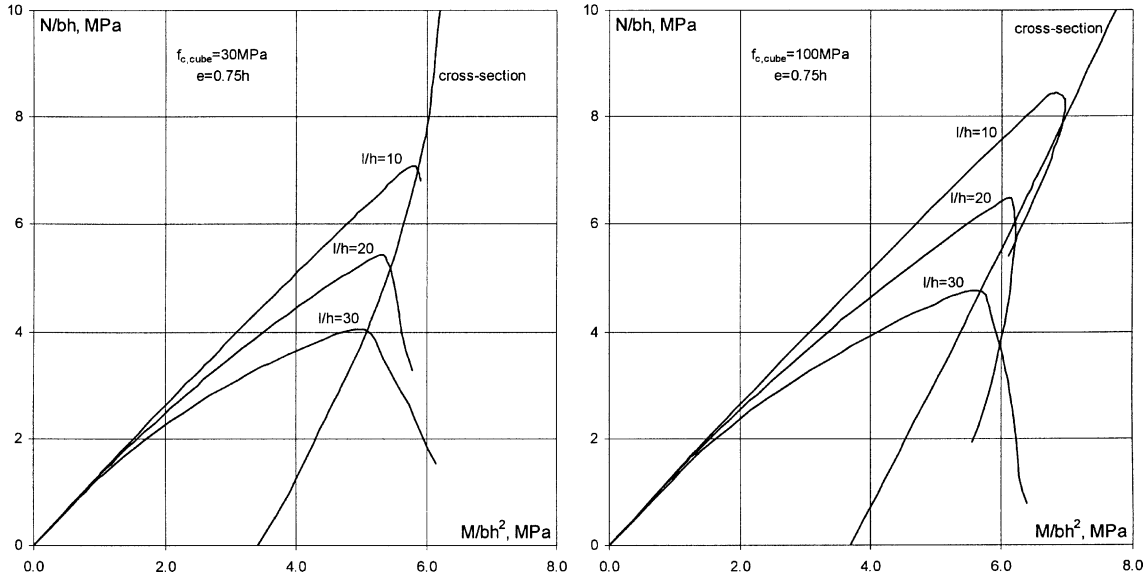

Fig. 21. Calculation analysis of load-bearing capacity of columns, $e = 0.75h$.

- In reinforced concrete elements, concrete shows maximum strains distinctly exceeding strains obtained from cylindrical specimens; the character of the destruction remains, however, abrupt.
- Concrete exhibits very good bond with reinforcement, also at large strains in tension zone.
- Limit curvatures of elements under bending do not differ from those in ordinary concrete for same reinforcement ratio.
- There is no reason to restrict the degree of redistribution of internal forces more than in the case of ordinary concrete.
- Higher degrees of minimum reinforcement are required because of greater f_{ctm}; this problem is well reflected in CEB [1] proposal.
- The behaviour of slender columns under immediate load does not also differ from the behaviour of ordinary concrete columns; failure through loss of stabil-

ity can occur in ordinary concrete columns as well as in HSC columns.

Acknowledgements

Thanks to the financial assistance of Research Grant No. 7 T07E with funds given by the Polish State Committee for Scientific Research for the development of this research. This research project is part of a long-term research programme on HSC members at Technical University of Lodz, Poland.

References

[1] CEB, High Performance Concrete, Recommended to the Model Code 90, Research Need, Bull d'Information No 228; 1995.
[2] Eurocode 2: Design of concrete structures. Part 1. General rules and rules for buildings; July 1999.
[3] Pendyala R, Mendis P, Patnaikuni I. Full-range behavior of high-strength concrete flexural members: comparison of ductility parameter of high and normal-strength concrete members, ACI Struct J, 1996;(January–February):30–5.
[4] Pecce M, Fabbrocino G. Plastic rotation capacity of beams in normal and high-performance concrete, ACI Struct J, 1999;(March–April):290–6.
[5] Fabbrocino G, Pecce M. Experimental analysis of influence of flexure – shear interaction on the rotation capacity of HPC beams. In: Proceedings of the 5th International Symposium on Utilization of High Strength/High Performance Concrete, vol. I, 1999 Jun; Norway (Sandefjord). p. 243–52.
[6] Weiss WJ, Guler K, Shah SP. An experimental investigation to determine the influence of size on the flexural behavior of high strength reinforced concrete beams, In: Proceedings of the 5th International Symposium on Utilization of High Strength/High Performance Concrete, vol. I, 1999 Jun; Norway (Sandefjord). p. 709–18.
[7] Kaminska ME. Doswiadczalne badania zelbetowych slupow ukosnie mimosrodowo sciskanych (Experimental Investigations of RC Columns under Biaxial Bending), Zeszyt 7, Wydawnictwo Katedry Budownictwa Betonowego Politechniki Lodzkiej, Lodz; 1995.
[8] Kaminska M, Czkwianianc A. Badania monolitycznych ram portalowych obciazonych silami pionowymi lub poziomymi (Tests of RC Portal Frames Subjected to Vertical or Lateral Force), Zeszyt 2, Wydawnictwo Katedry Budownictwa Betonowego Politechniki Lodzkiej, Lodz; 1993.
[9] Kaminska ME. Experimental research on HSC one-dimensional members, Zeszyt 8, Wydawnictwo Katedry Budownictwa Betonowego Politechniki Lodzkiej, Lodz; 1999.
[10] Naaman AE, Harajli MH, Wight JK. Analysis of ductility in partially prestressed concrete flexural members, PCI J 1986;(May–June): 64–87.
[11] Building Code Requirements for Structural Concrete (ACI 318-99) and Commentary (ACI 318R-99).
[12] Czkwianianc A, Kaminska M. Metoda nieliniowej analizy zelbetowych elementow pretowych (Method of nonlinear analysis of one-dimensional reinforced concrete members), PAN KILiW, IPPI, Studia z zakresu Inzynierii nr 36, Warszawa; 1993.